

# Differential functions of G protein and Baz–aPKC signaling pathways in *Drosophila* neuroblast asymmetric division

Yasushi Izumi, Nao Ohta, Asako Itoh-Furuya, Naoyuki Fuse, and Fumio Matsuzaki

Laboratory for Cell Asymmetry, Center for Developmental Biology, Institute of Physical and Chemical Research, and CREST, Japan Science and Technology Corporation, Kobe 650-0047, Japan

**D***rosophila melanogaster* neuroblasts (NBs) undergo asymmetric divisions during which cell-fate determinants localize asymmetrically, mitotic spindles orient along the apical–basal axis, and unequal-sized daughter cells appear. We identified here the first *Drosophila* mutant in the  $G\gamma 1$  subunit of heterotrimeric G protein, which produces  $G\gamma 1$  lacking its membrane anchor site and exhibits phenotypes identical to those of *G $\beta 13F$* , including abnormal spindle asymmetry and spindle orientation in NB divisions. This mutant fails to bind *G $\beta 13F$*  to the membrane, indicating an essential role of cortical  $G\gamma 1$ –*G $\beta 13F$*  signaling

in asymmetric divisions. In *G $\gamma 1$*  and *G $\beta 13F$*  mutant NBs, Pins– $G\alpha i$ , which normally localize in the apical cortex, no longer distribute asymmetrically. However, the other apical components, Bazooka–atypical PKC–Par6–Inscuteable, still remain polarized and responsible for asymmetric Miranda localization, suggesting their dominant role in localizing cell-fate determinants. Further analysis of *G $\beta\gamma$*  and other mutants indicates a predominant role of Partner of Inscuteable– $G\alpha i$  in spindle orientation. We thus suggest that the two apical signaling pathways have overlapping but different roles in asymmetric NB division.

## Introduction

Asymmetric cell division is a fundamental process that produces two daughter cells that differ in fate and size during development (Horvitz and Herskowitz, 1992). *Drosophila melanogaster* neural progenitor cells called neuroblasts (NBs) have been an excellent model for understanding the molecular mechanisms of asymmetric cell division (Matsuzaki, 2000; Doe and Bowerman, 2001; Jan and Jan, 2001; Knoblich, 2001; Chia and Yang, 2002). NBs delaminate from the neuroectoderm and repeatedly undergo asymmetric cell division that generates a larger apical NB and a smaller basal ganglion mother cell (GMC; Campos-Ortega, 1995). Neural cell-fate determinants such as Prospero and Numb segregate exclusively to the GMC, resulting in asymmetric gene expression patterns in the daughter cells (Rhyu et al., 1994; Hirata et al., 1995; Knoblich et al., 1995; Spana and Doe, 1995). Unequal partition of these determinants involves two elementary steps: (1) asymmetric localization of

Prospero and Numb to the basal cortex by associating with their respective adaptor proteins, Miranda and Partner of Numb (Ikeshima-Kataoka et al., 1997; Shen et al., 1997; Lu et al., 1998); and (2) reorientation of the mitotic spindle, which initially forms perpendicular to the apical–basal axis and then rotates 90° to ensure unequal partition of the basal determinants (Kraut et al., 1996; Kaltschmidt et al., 2000). Cell-size asymmetry in the NB daughter cells results from the basal deviation of the cleavage furrow, which is caused by generation of the asymmetric central spindle and its basal displacement (Chia and Yang, 2002; Kaltschmidt and Brand, 2002).

These asymmetric features of NB division are controlled by an apically localized multiprotein complex, which includes members of two signaling pathways that are distributed in different epithelial membrane compartments before NB delamination. One is an evolutionarily conserved signaling cassette consisting of Par-3 (called Bazooka [Baz]; Kuchinke et al., 1998; Schober et al., 1999; Wodarz et al., 1999), *Drosophila* Par-6 (DmPar-6; Petronczki and Knoblich, 2001), and *Drosophila* atypical PKC (DaPKC;

The online version of this article contains supplemental material.

Address correspondence to Fumio Matsuzaki, Laboratory for Cell Asymmetry, Center for Developmental Biology, RIKEN, 2-2-3 Minatojima-Minamimachi, Chuou-ku, Kobe 650-0047, Japan. Tel.: 81-78-306-3217. Fax: 81-78-306-3215. email: fumio@cdb.riken.go.jp

Key words: epithelium; cell polarity; heterotrimeric G protein; spindle orientation; *Drosophila melanogaster*

Abbreviations used in this paper: Baz, Bazooka; DaPKC, *Drosophila* atypical PKC; DmPar-6, *Drosophila* Par-6; GMC, ganglion mother cell; Insc, Inscuteable; NB, neuroblast; Pins, Partner of Inscuteable.

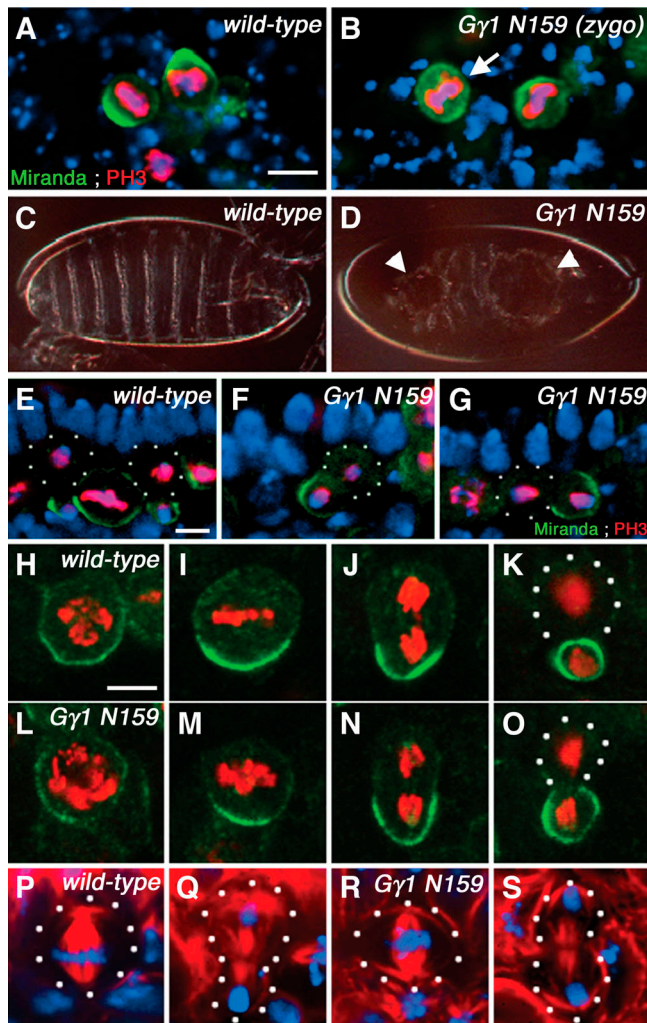


**Figure 1. Characterization of  $G\gamma 1^{N159}$  mutant.** (A and B) Zygotic phenotype of  $G\gamma 1^{N159}$  mutants. Stage-15 embryos of wild-type (A) and  $G\gamma 1^{N159}$  zygotic mutant (B) were stained for Miranda (green), phosphohistone H3 (red), a mitosis marker, and DNA (TOTO-3, blue). At late embryonic stages, wild-type mitotic NBs (A) still localize Miranda in a well-defined crescent, whereas NBs tends to localize Miranda uniformly along the cell cortex or in the cytoplasm in the  $G\gamma 1^{N159}$  zygotic mutant (B, arrow). (C and D) Cuticles of wild-type (C) and  $G\gamma 1^{N159}$  mutant (D) embryos.  $G\gamma 1^{N159}$  embryos showed characteristic anterior and posterior holes (arrowheads). (E–G) Wild-type (E) and  $G\gamma 1^{N159}$  mutant (F and G) embryos stained for Miranda (green), DNA (TOTO-3; blue) and phosphohistone H3 (red). Although wild-type NBs (E) divide perpendicular to the embryonic surface, the division axis in  $G\gamma 1^{N159}$  mutant NBs (F and G) becomes randomized, causing divisions at an oblique angle (F) or parallel (G) to the surface. Apical is up. (H–O) Wild-type (H–K) and  $G\gamma 1^{N159}$  mutant (L–O) NBs were stained for Miranda (green) and phosphohistone H3 (red); prophase (H and L), metaphase (I and M), anaphase (J and N), and telophase (K and O). In contrast to the wild-type, the  $G\gamma 1^{N159}$  mutant NBs cleave into nearly equal-sized daughter cells with one daughter inheriting Miranda. (P–S) Wild-type (P and Q) and  $G\gamma 1^{N159}$  mutant (R and S) NBs stained for DNA (TOTO-3; blue) and  $\alpha$ -tubulin (red) at metaphase (P and R), and telophase (Q and S). The Miranda crescents are oriented toward the bottom in H–S, although NBs in  $G\gamma 1^{N159}$  mutant embryos divide in random orientations. Miranda staining is not depicted for P–S for better visualization of microtubule organization. The ratios of the distances of the centrosome from the cleavage plane (NB/GMC) are: wild-type,  $2.19 \pm 0.47$  ( $n = 30$ );  $G\gamma 1^{N159}$ ,  $1.16 \pm 0.13$  ( $n = 23$ ). Bars, 5  $\mu\text{m}$ .

Wodarz et al., 2000), which localizes to the subapical region of the adherens junction in neuroepithelial cells (Knust and Bossinger, 2002). The other includes the  $\alpha$  subunit ( $G\alpha i$ ) of heterotrimeric G protein (Schaefer et al., 2001) and its guanine nucleotide dissociation inhibitor called Partner of Inscuteable (Pins; Parmentier et al., 2000; Schaefer et al., 2000; Yu et al., 2000), which distributes laterally in epithelia. At delamination, NBs begin to express the founding member of the apical complex, Inscuteable (Insc), which integrates these two signaling groups into the apical cortex by associating with both Pins and Baz (Kraut and Campos-Ortega, 1996; Kraut et al., 1996).

Mutations in the known apical component genes more or less affect both spindle orientation and the localization of the determinants at NB division. In contrast, cell-size asymmetry is not severely affected in mutants for any single apical component. This difference in the effects of apical mutations turned out to be due to redundant functions of the two apical signals in promoting daughter cell size asymmetry (Cai et al., 2003). The Baz–DaPKC–DmPar-6–Insc complex and the Pins– $G\alpha i$  complex can independently localize to create spindle asymmetry.

Recent findings revealed that the  $G\beta$  subunit ( $G\beta 13F$ ) of heterotrimeric G protein, which uniformly distributes along the NB cortex, also participates in the formation of unequal-sized daughters (Fuse et al., 2003; Yu et al., 2003). Its elimination results in a large symmetric spindle in random orientations causing division into nearly equal-sized cells, but the cell-fate determinants localize over one spindle pole to segregate into the GMC, indicating unique roles of  $G\beta 13F$  signaling in asymmetric NB division. Although defective localization of the apical components has been described for  $G\beta 13F$  mutants (Fuse et al., 2003; Yu et al., 2003), the relationship between the apical complex and  $G\beta 13F$  signaling is not understood well enough to explain their phenotypic differences. In addition, these findings raise a fundamental question of whether the two apical signaling pathways have differential or equivalent roles in basal protein localization and spindle orientation; this question has not been answered definitively.

In this paper, we document the first mutant for the  $G\gamma 1$  gene encoding one of two *Drosophila*  $G\gamma$  subunits of heterotrimeric G protein (Ray and Ganguly, 1992, 1994; Schulz et al., 1999). This  $G\gamma 1^{N159}$  mutant, which produces a truncated  $G\gamma 1$ , fails to localize  $G\beta 13F$  to the cortex and shows essentially the same phenotype as the loss of function mutant of  $G\beta 13F$ .  $G\gamma 1$  is required for localizing  $G\beta 13F$  to the NB cortex, presumably as its binding partner, indicating the essential role of cortical  $G\beta 13F$ – $G\gamma 1$  signaling in the induction of asymmetry in daughter cell size. We also found that, in both  $G\gamma 1$  and  $G\beta 13F$  mutants, NBs retain asymmetric localization of the Baz–DaPKC–DmPar-6–Insc complex but not of Pins– $G\alpha i$ . This localized Baz activity is responsible for Miranda localization and the residual asymmetry in NB daughter cell size in these mutants. These observations led us to reexamine the roles of the apical components, and we found evidence indicating distinct requirements for apical components in the two important processes for asymmetric NB division. Baz–DaPKC–DmPar-6 are crucial for asymmetric localization of the cell-fate

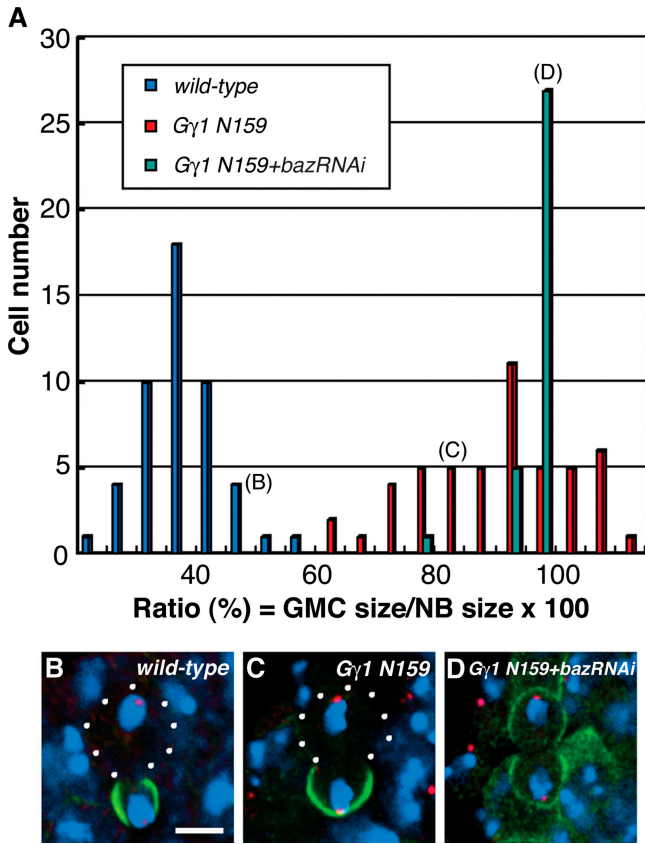


**Figure 2. Sizes of daughter cells resulting from division of *Gγ1<sup>N159</sup>* mutant and wild-type NBs.** (A) Relative sizes of GMC and sibling NB at the first cell division in wild-type (blue), *Gγ1<sup>N159</sup>* mutant (red), and *Gγ1<sup>N159</sup>* mutant embryos injected with *baz* dsRNA (green). (B–D) Telophase NBs in wild-type (B), *Gγ1<sup>N159</sup>* embryos (C), and *Gγ1<sup>N159</sup>* embryos injected with *baz* dsRNA (D), which were stained for Miranda (green),  $\gamma$ -tubulin (red), and DNA (TOTO-3; blue). In the *Gγ1<sup>N159</sup>* mutant, NBs localize Miranda in the crescent to segregate it into the GMC, which is slightly smaller than the sibling NB (C). Inhibition of *baz* activity (by RNAi) in *Gγ1<sup>N159</sup>* mutant embryos results in complete loss of cell-size asymmetry and uniform Miranda distribution (D). The cell size ratios (GMC/NB) for dividing NBs in B–D are 50%, 81%, and 97%, respectively, and are marked in A. Bar (B–D), 5  $\mu$ m.

determinants, and Pins–G $\alpha$ i mainly control spindle orientation. We suggest that the two apical signaling pathways play overlapping but distinct roles in the asymmetric division of NBs.

## Results

### NBs divide into nearly equal-sized daughters in *N159* mutant

We identified a zygotic lethal mutation *N159* that affects Miranda distribution in late-stage embryos (stages 15–16), by a mutational screen using Miranda as a polarity marker (Fig. 1, A and B; see Materials and methods). In the *N159* zygotic mutant, abnormal Miranda distribution is observed only in late embryonic stages, suggesting a strong maternal contribution of the mutated gene. We examined embryos from *N159* germline clones, which are maternally and zygotically homozygous for *N159* (hereafter called the *N159* mu-

**Table 1. Diameters of daughter cells resulting from NB cell divisions<sup>a</sup>**

Genotype	GMC	NB	GMC/NB <sup>b</sup>
	$\mu$ m	$\mu$ m	%
Wild type ( $n = 50$ )	$4.2 \pm 0.6$	$11.2 \pm 1.2$	$37.7 \pm 6.8$
<i>Gγ1<sup>N159</sup></i> ( $n = 50$ )	$7.8 \pm 1.0$	$8.7 \pm 1.0$	$89.1 \pm 12.8$
<i>Gβ13F<sup>-</sup></i> ( $n = 50$ )	$8.0 \pm 0.8$	$8.9 \pm 1.0$	$90.2 \pm 8.0$
<i>Gγ1<sup>N159</sup></i> + <i>baz</i> dsRNA ( $n = 33$ )	$7.7 \pm 1.0$	$8.0 \pm 0.9$	$96.0 \pm 3.7$

<sup>a</sup>The diameters of GMCs (which inherit Miranda) and NBs (which do not inherit Miranda) in telophase NBs of stage 9 embryos were measured for each genotype. Cell contours of telophase NBs were traced by Miranda staining, which outlined not only the budding GMC but also the NB part. For *Gγ1<sup>N159</sup>* germline clone embryos injected with *baz* dsRNA (*Gγ1<sup>N159</sup>* + *baz* dsRNA), the larger daughter cell was assumed to be the NB. Data are means  $\pm$  SD.

<sup>b</sup>Ratio of the diameter of GMC relative to its sibling NB.

tant). The *N159* mutant exhibits abnormal gastrulation (Fig. 1, C and D). The apical–basal polarity of the mutant epithelial cell is virtually normal, as indicated by the distributions of DE-cadherin, Baz, and neurotactin, (unpublished data). However, the *N159* mutation randomizes spindle orientation (Fig. 1, E–G) and affects cell-size difference in the daughter cells from the initial NB division. Although mutant NBs localize Miranda in the crescent to segregate it into the GMC (95%,  $n = 69$ ), the cell size ratio of the GMC relative to its sibling NB increases remarkably, compared with that in wild-type divisions (Table 1; Fig. 1, H–O; Fig. 2, A and C).

As expected from the equalized daughter cell size (Fuse et al., 2003), microtubule structures in the mutant NBs become nearly symmetric and develop well from both centrosomes throughout mitosis (Fig. 1, R and S), in contrast to wild-type mitotic NBs that develop apically biased microtubules (Fig. 1, P and Q). All these characteristics of the *N159* mutant are indistinguishable from those of the null mutants for *Gβ13F* (Schaefer et al., 2001; Fuse et al., 2003; Yu et al., 2003). *N159* NBs show aberrant localization of Miranda at late embryonic stages, as observed in zygotic *N159* mutants as well as in *Gβ13F* mutants (Fuse et al., 2003).

### *N159* is a mutation of the *Gγ1* gene

*N159* turned out to include a nonsense mutation in the *Gγ1* gene (Ray and Ganguly, 1992, 1994). The mutant *Gγ1* gene produces a truncated protein lacking the COOH-terminal isoprenylation site that acts in membrane anchoring (Fig. 3 A; see Materials and methods). *N159* indeed fails to complement a P-insertion allele of *Gγ1* (K08017). Expression of a wild-type *Gγ1* transgene rescues the *N159* mutant phenotypes with respect to gastrulation (unpublished data), daughter cell size (Fig. S1 A, available at <http://www.jcb.org/cgi/content/full/jcb.200309162/DC1>), and spindle orientation (Fig. S1 C), as well as in the localization of the apical components (Fig. S1 B; see Fig. 4), indicating that the *N159* characteristics originate from the mutated *Gγ1* gene; we call this allele *Gγ1<sup>N159</sup>*. In situ hybridization revealed a high maternal contribution in early embryos and subsequent uniform expression of *Gγ1* (Fig. 3 B). The other *Gγ* gene, *Gγ30A*, is not expressed in early embryos (unpublished data).



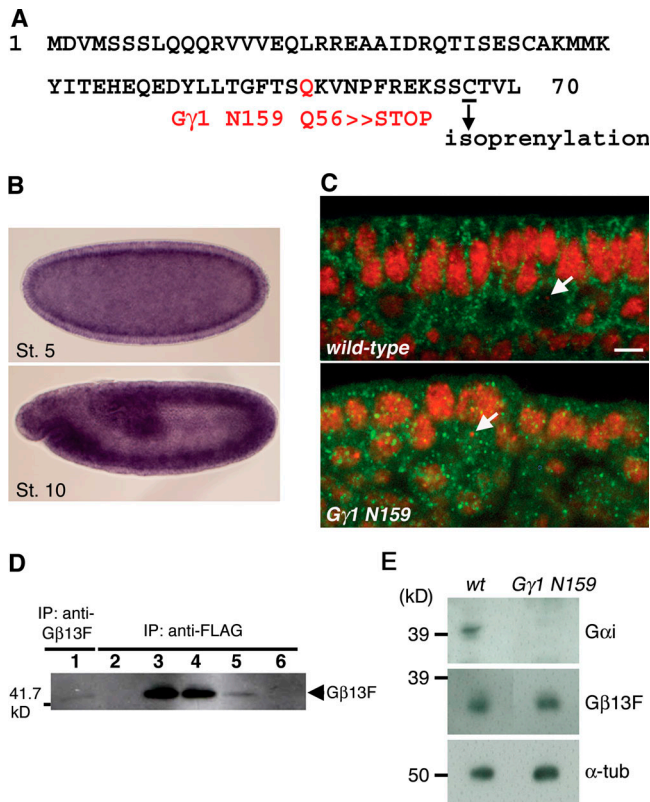


**Figure 3. Evidence that N159 is a mutation of the G $\gamma$ 1 gene.** (A) The N159 mutation is a single C to T nucleotide change that inserts a stop codon at the position of amino acid 56 of the G $\gamma$ 1 subunit of G protein. The truncated sequence includes the amino acid that is isoprenylated (underlined) and which is needed to target the G $\beta\gamma$  complex to the cell membrane. (B) In situ hybridization with a G $\gamma$ 1 probe. G $\gamma$ 1 transcripts are abundant in early embryonic stages (stage 5). G $\gamma$ 1 is ubiquitously expressed throughout embryogenesis (as observed at stage 10). (C) Localization of G $\beta$ 13F in the G $\gamma$ 1<sup>N159</sup> mutant. Stage-9 embryos were stained with anti-Cen190 antibody (red), to reveal nuclei and centrosomes, and with anti-G $\beta$ 13F antibody (green). In wild-type NBs and epithelial cells, G $\beta$ 13F is mainly distributed throughout the cell cortex (top). In G $\gamma$ 1<sup>N159</sup> embryos, G $\beta$ 13F fails to localize to the cell cortex (bottom). Arrows indicate the centrosomes of metaphase NBs, which are stained for Cen190. Apical is toward the top. Bar, 5  $\mu$ m. (D) Co-immunoprecipitation of G $\gamma$ 1 and G $\beta$ 13F. G $\beta$ 13F is immunoprecipitated from an extract of wild-type embryos by anti-G $\beta$ 13F antibody (lane 1). G $\beta$ 13F is also immunoprecipitated by anti-FLAG antibody from an extract of embryos expressing FLAG-tagged G $\gamma$ 1 (lane 3) or FLAG-tagged G $\gamma$ 1C67S (lane 4, a G $\gamma$ 1 mutant protein defective in COOH-terminal isoprenylation) or FLAG-tagged G $\gamma$ 1<sup>N159</sup> (lane 5). G $\beta$ 13F is not immunoprecipitated from wild-type embryos (lane 2) or from embryos expressing FLAG-tagged Miranda (lane 6). Anti-G $\beta$ 13F antibody was used for the Western blot. (E) Western blots of protein extracts prepared from wild-type embryos (wt) or embryos from G $\gamma$ 1<sup>N159</sup> germline clones (G $\gamma$ 1 N159). In the mutant embryos, G $\alpha$ i levels are strongly decreased (top), but G $\beta$ 13F (middle) and  $\alpha$ -tubulin (bottom) levels are unchanged.

### G $\gamma$ 1 is required for proper localization of G $\beta$ 13F

We examined the subcellular distribution of G $\beta$ 13F in G $\gamma$ 1<sup>N159</sup> embryos because the mutant G $\gamma$ 1 should lack the membrane-binding site. In wild-type NBs and epithelial cells, G $\beta$ 13F is distributed mainly in the cell cortex (Fig. 3 C). In the G $\gamma$ 1<sup>N159</sup> mutant cells, it is distributed to the cytoplasm, often in a punctate manner (Fig. 3 C). G $\gamma$ 1 transgene

expression, which rescues the mutant phenotype, restores the cortical localization of G $\beta$ 13F in the G $\gamma$ 1<sup>N159</sup> mutant (Fig. S1 D). This restoration is observed neither in G $\gamma$ 1<sup>N159</sup> mutant embryos expressing the G $\gamma$ 1C67S mutant gene (defective in COOH-terminal isoprenylation) nor in mutant embryos expressing the G $\gamma$ 1<sup>N159</sup> transgene itself (Fig. S1 D; see Materials and methods). Therefore, the COOH-terminal isoprenylation site of G $\gamma$ 1 is indispensable for the cortical localization and cellular function of G $\beta$ 13F.

We also performed immunoprecipitation of extracts from wild-type embryos expressing FLAG-tagged G $\gamma$ 1 with anti-FLAG antibodies and found that G $\beta$ 13F coimmunoprecipitated with G $\gamma$ 1 (Fig. 3 D, lane 3) but it did not for control embryos (Fig. 3 D, lanes 2 and 6). This result, together with the essential role of G $\gamma$ 1 in recruiting G $\beta$ 13F to the membrane, suggests that G $\gamma$ 1 is an in vivo binding partner of G $\beta$ 13F. We note that the association of G $\beta$ 13F with G $\gamma$ 1 does not appear to require the isoprenylation site of G $\gamma$ 1 because both the G $\gamma$ 1C67S (Fig. 3 D, lane 4) and G $\gamma$ 1<sup>N159</sup> (Fig. 3 D, lane 5) proteins coimmunoprecipitated with G $\beta$ 13F. We could not determine the distribution of G $\gamma$ 1 because of a lack of suitable antibodies. However, G $\gamma$ 1 and G $\beta$ 13F most likely colocalize in the cell cortex, because G $\beta$ 13F localization depends completely on the ability of G $\gamma$ 1 to bind to membranes.

### Differential effects of G $\gamma$ 1–G $\beta$ 13F on the asymmetric localization of Pins–G $\alpha$ i and Baz–DaPKC–DmPar-6–Insc

The asymmetric localization of Miranda and the residual difference in daughter cell sizes in the G $\gamma$ 1<sup>N159</sup> mutant NBs indicate that some cell polarity remains in these NBs. The null G $\beta$ 13F mutant shows similar residual cell asymmetry, which depends on baz activity (Table I; Fuse et al., 2003; Yu et al., 2003). We examined whether the residual asymmetry in the G $\gamma$ 1<sup>N159</sup> mutant depends on baz activity and found that elimination of baz activity (by RNAi) in G $\gamma$ 1<sup>N159</sup> results in complete loss of cell-size asymmetry and in uniform Miranda distribution (Fig. 2 A, D). These polar effects of Baz suggest asymmetric distribution of some apical components in the G $\gamma$ 1<sup>N159</sup> and G $\beta$ 13F mutants, which prompted us to carefully reexamine the distribution of the apical components.

In wild-type NBs, apical components localize in the apical cortical crescent (Fig. 4, A, D, G, J, M, and P). In G $\gamma$ 1<sup>N159</sup> NBs, Pins is distributed uniformly throughout the cell cortex and in the cytoplasm of all metaphase NBs (100%,  $n = 27$ ; Fig. 4 B). G $\alpha$ i becomes undetectable at early embryonic stages (Fig. 4 E). The degradation of G $\alpha$ i was confirmed by Western blotting of G $\gamma$ 1<sup>N159</sup> mutant embryos (Fig. 3 E), suggesting that stability of G $\alpha$ i depends on the presence of the cortical G $\beta$ 13F–G $\gamma$ 1 complex. Other apical components, Insc, Baz, DmPar-6, and DaPKC, also no longer distribute normally in G $\gamma$ 1<sup>N159</sup> NBs. Their staining intensity is decreased. However, we found that their distribution remains asymmetric in the majority of metaphase NBs; Insc distributes diffusely but still asymmetrically in the cytoplasm and cell cortex (Fig. 4 H; 75% of NBs localizing Miranda,  $n = 60$ ). Baz (Fig. 4 K), DmPar-6 (Fig. 4 N), and DaPKC (Fig. 4 Q; 84% of NBs localizing Miranda,  $n = 56$ ) form cortical crescents. The polarized distribution of DmPar-6 and DaPKC is more evident at the end of cytokinesis, even in di-

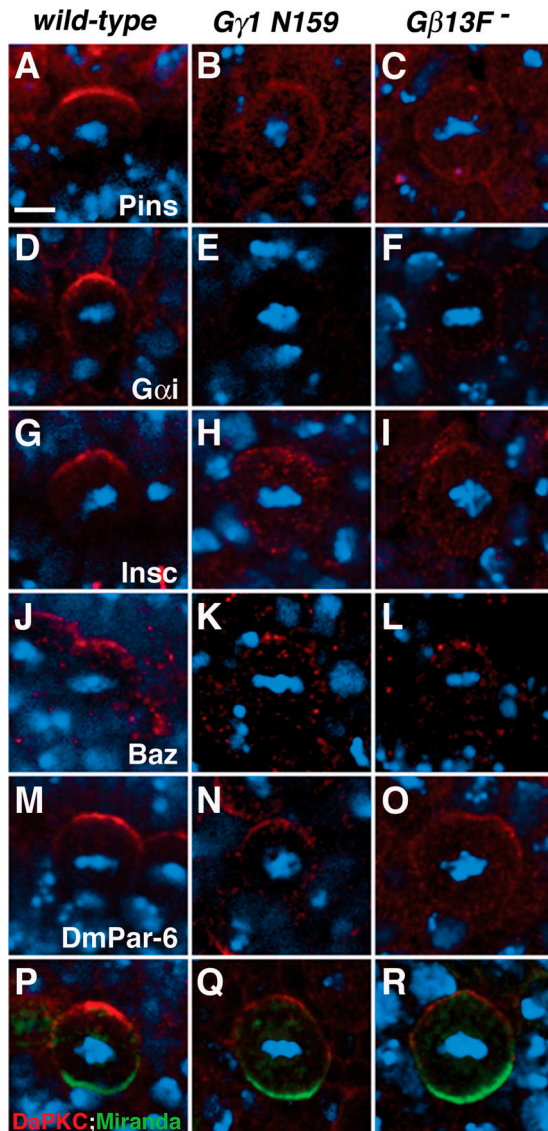


**Figure 4. Localization of apical components in metaphase NBs in  $G\gamma 1^{N159}$  and  $G\beta 13F$  mutants.** Localization of the apical components in mitotic NBs in the wild-type (A, D, G, J, M, and P),  $G\gamma 1^{N159}$  mutant (B, E, H, K, N, and Q), and  $G\beta 13F$  mutant (C, F, I, L, O, and R). Stage-9 embryos were stained for Pins (A–C),  $G\alpha i$  (D–F), Insc (G–I), Baz (J–L), DmPar-6 (M–O), DaPKC (P–R, red), and Miranda (green), as well as for DNA (blue). The Miranda crescents are oriented toward the bottom but are shown only in P–R (green). In  $G\gamma 1^{N159}$  and  $G\beta 13F$  mutant NBs, Pins distributes all around the cell cortex, as well as in the cytoplasm (B and C),  $G\alpha i$  is not detectable (E and F), Insc distribution is less polarized in the cytoplasm and the cell cortex (H and I) than in the wild type; and Baz (K and L), DmPar-6 (N and O), and DaPKC (Q and R) form cortical crescents, although the intensity of antibody staining is less than in the wild type. Bar (A–R), 5  $\mu$ m.

visions producing two equal-sized daughters (Fig. S2, available at <http://www.jcb.org/cgi/content/full/jcb.200309162/DC1>). DaPKC (87% of telophase NBs,  $n = 30$ ) and DmPar-6 (unpublished data) remain in the daughter NB but are excluded from the sibling GMC, as also observed in wild-type NB divisions (100%,  $n = 30$ ; Fig. S2, A and B). Interestingly, unlike DaPKC and DmPar-6, Insc is observed on both the NB and GMC sides in most telophase NBs in

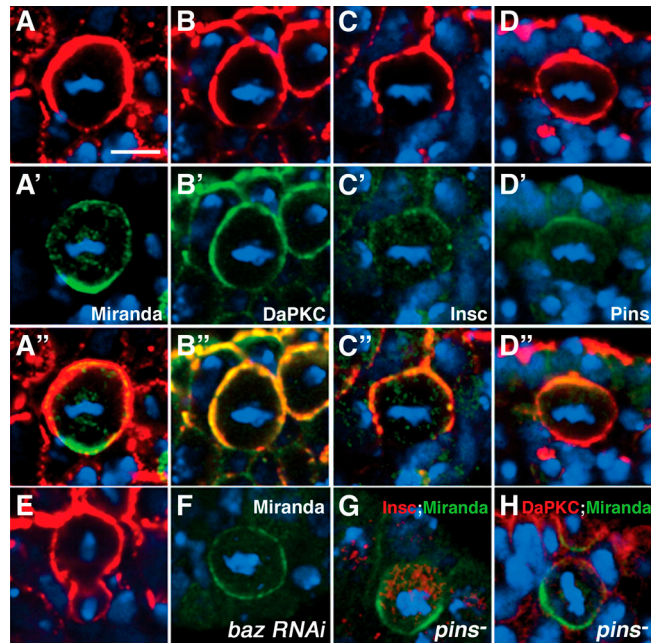


**Figure 5. Effect of *baz* overexpression on localization of Miranda.** (A–D) *baz*-overexpressing NBs were double-stained: red for Baz (A–D) and green for Miranda (A'), DaPKC (B'), Insc (C'), or Pins (D'). Merged images for each double staining are shown in A'', B'', C'', and D''. The overproduced Baz is not restricted to the apical cortex but is found more broadly in the lateral and basal cortex (A–C) or throughout the cortex (D). In these NBs, Miranda and Baz distribute in a complementary pattern (A and A'), DaPKC (B') and Insc (C') codistribute with Baz (B and C). However, Pins distribution (D') is restricted to the apical cortex regardless of the uniformly cortical localization of Baz (D). (E) *baz*-overexpressing NBs produce unequal-sized daughters even when Baz is distributed all over the cortex of both the prospective NB and GMC during cytokinesis. (F) Miranda distributes uniformly in the NB cortex in wild-type embryos injected with *baz* dsRNA. (G and H) Mitotic *pins* mutant NBs stained for Insc (G, red), DaPKC (H, red), and Miranda (G and H, green); 70% of NBs localize Miranda asymmetrically along the division axis, which is often misoriented. In *pins* mutant NBs, Insc localizes asymmetrically in the cytoplasm (G), and DaPKC forms a weak cortical crescent (H). Apical is up. DNA was stained with TOTO-3 (blue). Bar (A–H), 5  $\mu$ m.

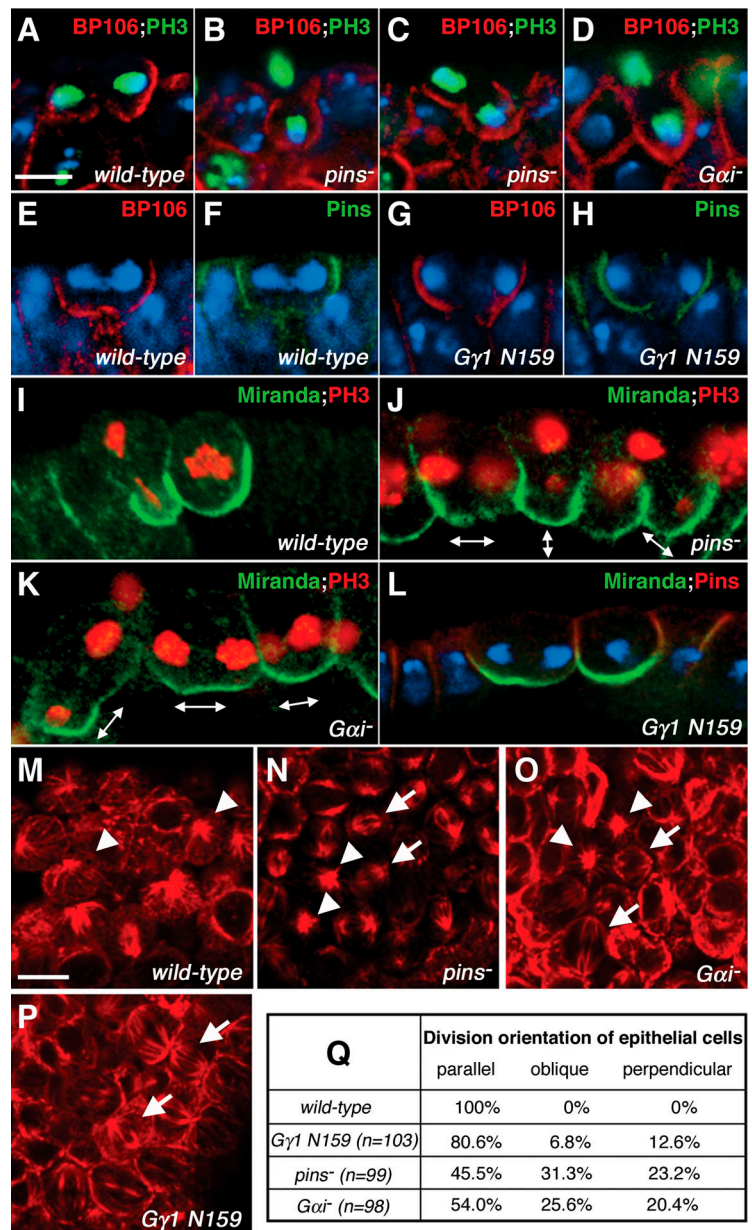
$G\gamma 1^{N159}$  mutants (Fig. S2 E). Elimination of  $G\beta 13F$  has the same effects on localization of the various apical components as the  $G\gamma 1^{N159}$  mutation does (Fig. 4; Fig. S2, C and F). Thus,  $G\beta\gamma$  signaling in NBs is necessary for asymmetric localization of  $G\alpha i$  and Pins but not of Insc, Baz, DmPar-6, or DaPKC. This remaining Baz–DaPKC pathway is responsible for asymmetric localization of the determinants and residual cell-size asymmetry in the absence of the  $G\beta\gamma$  signal, because elimination of *baz* activity in the  $G\gamma 1^{N159}$  background completely disrupts them (Fig. 2, C and D).

### Baz–DaPKC pathway directs asymmetric localization of cell-fate determinants

The Baz-dependent localization of Miranda when the distributions of  $G\alpha i$  and Pins are uniform (in the absence of  $G\beta 13F$ – $G\gamma 1$ ; Fig. 2 D) raises the possibility that the localization of cell-fate determinants is mainly regulated by the Baz–DaPKC pathway rather than the Pins– $G\alpha i$  pathway in wild-



**Figure 6. Effect of *pins* and G protein mutations on spindle orientation.** (A–D) Wild-type (A), *pins* (B and C), and *Gai* (D) mutant epithelial cells were stained for the membrane marker BP106 (red) and for phosphohistone H3 (green). BP106 is found in the lateral and basal membrane domains in epithelial cells but stains the entire cell contour in NBs. The apical surface of epithelial cells does not stain for BP106. The epithelial cells of *pins* and *Gai* mutants often divide perpendicular (B) or at an oblique angle (C and D) to the embryo's surface, but wild-type cells divide parallel to the surface (A). Apical is up. (E–H) Wild-type (E and F) and *Gγ1<sup>N159</sup>* mutant (G and H) epithelial cells were stained for BP106 (E and G, red), Pins (F and H, green), and DNA (blue). In both wild-type and *Gγ1<sup>N159</sup>* mutant epithelial cells Pins is localized in the lateral cortex and the cells divide parallel to the surface (F and H). Apical is up. (I–L) Mitotic domain 9 cells in wild-type (I), *pins* (J), *Gai* (K), and *Gγ1<sup>N159</sup>* (L) mutants were stained for Miranda (green) and phosphohistone H3 (red) in I–K or for Miranda (green), Pins (red), and DNA (blue) in L. Wild-type cells (I) in mitotic domain 9 divide perpendicular to the embryonic surface. Cells in the *pins* (J) and *Gai* (K) mutants divide not only perpendicular but also parallel or at an oblique angle to the surface. Mitotic domain 9 cells in the *Gγ1<sup>N159</sup>* mutant (L) localize Pins at the lateral cortex and divide parallel to the surface. Arrows show the orientations of divisions. Apical is up. (M–P) Surface views of mitotic domain 9 in wild-type (M), *pins* (N), *Gai* (O), and *Gγ1<sup>N159</sup>* (P) mutant embryos stained with anti- $\alpha$ -tubulin. Mitotic spindles are oriented perpendicular to the surface in the wild-type (M), parallel or perpendicular to the surface in the *pins* (N) and *Gai* (O) mutants, and parallel in the *Gγ1<sup>N159</sup>* mutant (P). Arrowheads indicate divisions perpendicular to the embryonic surface; arrows indicate divisions parallel to the surface. (Q) Quantitative measurements of the orientations of epithelial cell divisions in the wild-type, *pins*, *Gai*, and *Gγ1<sup>N159</sup>* mutants. *n* = number of telophase epithelial cells scored. Bars: (A–L) 5  $\mu$ m; (M–P) 10  $\mu$ m.



type NBs. To test this possibility, we modulated Baz distribution by overproducing Baz in the wild-type background and followed Miranda localization. In these NBs, Baz distributes more broadly, not only in the apical cortex but also in the lateral and basal cortex (Fig. 5, A–C; Wodarz et al., 1999, 2000) and is often uniformly distributed throughout the cortex (Fig. 5 D). Under this condition, DaPKC (Fig. 5 B'), DmPar-6 (unpublished data), and Insc (Fig. 5 C') are co-distributed with the ectopically distributing Baz as shown previously (Petronczki and Knoblich, 2001; Wodarz et al., 2000). In contrast, even when Baz is uniformly distributed around the cortex (Fig. 5, D and D'; unpublished data), Pins and G $\alpha$ i do not appear to change their normal asymmetric distribution, indicating that the polarized localization of the Pins–G $\alpha$ i complex is unaffected by the misdistributed Baz–DaPKC. Under this situation, Miranda redistributes in a complementary manner to Baz (Fig. 5, A and A'; 100% of metaphase NBs, *n* = 23). On the other hand, inhibition of *baz* (by

RNAi) in wild-type embryos results in uniform cortical distribution of Miranda (Fig. 5 F), without affecting the asymmetric distributions of Pins and G $\alpha$ i (unpublished data; Cai et al., 2003). Thus, both expansion and reduction of Baz distribution in the cortex alter Miranda localization so that Miranda is excluded from the area where Baz–DaPKC are localized and shows no correlation with Pins–G $\alpha$ i localization. We infer that the localization of cell-fate determinants is predominantly regulated by the Baz–DaPKC pathway. Consistent with this idea, polarized Miranda distribution itself is not strongly affected by a lack of Pins or G $\alpha$ i, although its crescent has been reported to misorient (Schaefer et al., 2000; Yu et al., 2000, 2003). In our observations, 70% of metaphase NBs in a *pins* null mutant (*n* = 80) show asymmetric localization of Miranda (Fig. 5, G and H). In these NBs, Insc distributes diffusely and asymmetrically in the cytoplasm (Fig. 5 G; 72% of NBs localizing Miranda, *n* = 46). Baz, DmPar-6, and DaPKC (Fig. 5 H; 90% of NBs localizing Miranda, *n* = 52)

form relatively weak crescents. Thus, asymmetric localization of the cell-fate determinants and Baz–DaPKC–DmPar-6 does not necessarily require Pins or G $\alpha$ i function.

Interestingly, NBs that overproduce Baz yield unequal-sized daughters, even when Baz is distributed nearly uniformly around the cortex of both the NB and the newly forming GMC during late cytokinesis (Fig. 5 E), suggesting that the Baz–DaPKC pathway does not severely affect cell-size asymmetry when Pins–G $\alpha$ i localize asymmetrically.

### Pins–G $\alpha$ i pathway predominantly regulates spindle orientation

Finally, we investigated the regulation of spindle orientation. In *pins* and *Gai* mutants, NBs show defects in spindle orientation (Schaefer et al., 2000; Yu et al., 2000, 2003). We found that epithelial cells also show defects in spindle orientation in these mutants. In wild-type embryos, epithelial cells divide parallel to the embryo's surface (Fig. 6, A, E, and F). In contrast, they often divide perpendicular (Fig. 6 B) or at an oblique angle (Fig. 6 C) to the embryo's surface in *pins* mutants (Fig. 6 Q). These observations suggest that the axis of division in mitotic epithelial cells is randomly oriented in *pins* mutants. In mitotic domain 9 of the procephalic neurogenic region, wild-type cells divide perpendicular to the surface, producing the smaller GMCs on the inner side (Fig. 6, I and M). It was reported that these cells divide parallel to the surface in *pins* mutants (Yu et al., 2000). However, our analysis indicates that the *pins* mutant cells in mitotic domain 9 divide in directions not only parallel but also perpendicular and often at an oblique angle to the embryonic surface (Fig. 6, J and N). Defects in the orientation of division are similarly observed in *Gai* mutants (Fig. 6, D, K, O, and Q). These results indicate that Pins and G $\alpha$ i are required for proper spindle orientation in both epithelial cells and mitotic domain 9 cells, as also observed in NBs (Yu et al., 2000).

In *G $\gamma$ 1* and *G $\beta$ 13F* mutants, Pins remains localized to the lateral cortex of epithelial cells (Fig. 6, G and H; unpublished data) and mitotic domain 9 cells (Fig. 6 L; unpublished data); G $\alpha$ i appears to diminish (unpublished data). In these mutants, most epithelial cells (Fig. 6, G, H, and Q) as well as mitotic domain 9 cells (Fig. 6, L and P) divide parallel to the surface. Thus, *G $\beta$ 13F* (and *G $\gamma$ 1*) mutations and *Pins* (and *G $\alpha$ i*) mutations affect spindle orientation differently, as summarized in Fig. 7 A. As long as Pins distributes asymmetrically in cells (mitotic domain 9 and epithelial cells in *G $\beta$*  or *G $\gamma$*  mutants), the spindle orients so that one or both spindle poles lie over the cortical domain where Pins distributes. However, spindles orient randomly when Pins (G $\alpha$ i) is distributed uniformly (in *G $\beta$*  and *G $\gamma$*  mutant NBs) or when Pins is absent (in epithelial cells, mitotic domain 9 cells, and NBs in *pins* mutants). These results can be interpreted as evidence that Pins–G $\alpha$ i activities direct a spindle pole to the region where Pins is localized. In wild-type NBs and mitotic domain 9 cells, apically localized Pins–G $\alpha$ i rotate the spindle into the apical–basal axis. But in wild-type epithelial cells or *G $\beta$ 13F*–*G $\gamma$ 1* mutant mitotic domain 9 cells, laterally localized Pins–G $\alpha$ i maintain the spindle parallel to the embryo's surface.

Together, our results suggest that Pins–G $\alpha$ i principally regulate spindle orientation, but not the localization of cell-fate determinants. The Pins–G $\alpha$ i and Baz–DaPKC path-

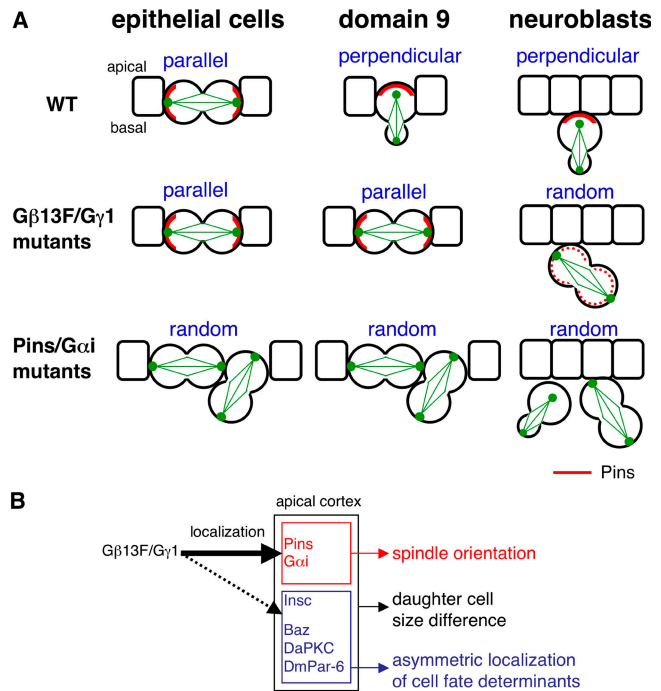


**Figure 7. Summary and model.** (A) Division orientation of epithelial cells and mitotic domain 9 cells (Fig. 6) is summarized together with that of NBs. Note that the spindle is always pointed to the localization of Pins. However, spindles orient randomly when Pins is uniformly distributed or absent. See Results and Discussion for details. (B) The two apical signaling pathways are differentially regulated by the G $\beta$ /G $\gamma$  signal and play overlapping but distinct roles in the asymmetric division of NBs. See Discussion for details.

ways appear to play different roles in processes leading to asymmetric segregation of the cell-fate determinants (Fig. 7 B), although they control the production of unequal-sized daughters in a redundant fashion.

## Discussion

In this paper, we analyzed the first *Drosophila* mutant for the *G $\gamma$ 1* subunit of heterotrimeric G protein and found that cortical signaling mediated by the G $\beta$ 13F–G $\gamma$ 1 complex is critical for creating cell-size asymmetry but not for localizing cell-fate determinants in asymmetric NB division. Our findings concerning differential effects of the G $\beta\gamma$  signal on the localization of the apical components led us to dissect the contributions of the two apical signaling pathways to other aspects of asymmetric NB division. As summarized in Fig. 7 B, we suggest that the Baz–DaPKC–DmPar-6–Insc complex and the Pins–G $\alpha$ i complex have different roles in regulating the cell-fate determinants and spindle orientation.

### Differential G $\beta\gamma$ signaling along the apical–basal axis in NBs

Because the G $\beta$ 13F–G $\gamma$ 1 complex, which distributes uniformly in the cortex, functions in asymmetric organization of the spindle, differential activation or inactivation of G $\beta\gamma$  signaling must occur in the apical–basal direction. A recent work revealed that two apical signaling pathways are implicated in the apical–basal difference in spindle development



in a redundant fashion (Cai et al., 2003). What is the relationship between the apical signals and the G $\beta$  $\gamma$  signal? Spindle size is reduced by an increase in the amount of G $\beta$  $\gamma$ , but a lack of G $\beta$  $\gamma$  results in formation of a large, symmetric spindle (Fig. 1; Fuse et al., 2003). These findings raise the possibility that spindle development is suppressed by the G $\beta$  $\gamma$  signal, which is repressed by the presence of an apical complex on the apical side in the wild-type cells, resulting in a large apical and small basal spindle. This model suggests that the apical complex acts upstream of the G $\beta$  $\gamma$  signal. On the other hand, elimination of G $\beta$ 13F affects the localization of the apical components: Pins becomes uniformly distributed and G $\alpha$ i becomes undetectable. In addition, *G $\gamma$ 1<sup>N159</sup>* and *G $\beta$ 13F* mutations appear to destabilize the localization of the components in the Baz–DaPKC pathway, as judged by the reduced staining by their antibodies (although this may be an indirect consequence of the mislocalization of Pins–G $\alpha$ i). The G $\beta$  $\gamma$  signal is thus required for normal distribution of the components of both apical pathways, consistent with the idea that the apical pathways acts downstream of the G $\beta$  $\gamma$  signal in regulating spindle asymmetry (Yu et al., 2003). Tests for epistasis between the apical pathways and the G $\beta$  $\gamma$  signal are needed to clarify their relationship in the regulation of spindle organization.

#### Dosage effects of apical components and the role of Insc

The effects of *G $\gamma$ 1<sup>N159</sup>* and *G $\beta$ 13F* mutations (this paper; Fuse et al., 2003) on cell-size asymmetry are remarkable but different from those in double mutants in which both apical pathways are disrupted simultaneously, where daughter cell sizes are completely equal (Cai et al., 2003; Yu et al., 2003). The cell-size ratio of GMCs to their sibling NBs shows a broad distribution: from 0.6 to 1 in the *G $\gamma$ 1* (and *G $\beta$ 13F*) mutants (Fig. 2 A). This residual asymmetry in daughter cell size is due to Baz–DaPKC activity (Fig. 2, Fuse et al., 2003; Yu et al., 2003). Here, we showed that the components of this pathway indeed distribute asymmetrically in *G $\gamma$ 1* (and *G $\beta$ 13F*) mutant NBs in which Pins–G $\alpha$ i activity is no longer asymmetric (Pins is uniformly distributed and G $\alpha$ i is absent).

Why does this polarized Baz–DaPKC activity cause less asymmetry in daughter cell size in spite of the redundant function of the Baz–DaPKC pathway and Pins–G $\alpha$ i? Antibody staining for Baz, DaPKC, and DmPar-6 suggests that their levels and their polarized distribution are weakened in *G $\gamma$ 1* (and *G $\beta$ 13F*) mutants. A possible explanation is that low levels of polarized Baz–DaPKC activity confer only low levels of asymmetry to the daughter cell size in the absence of polarized Pins–G $\alpha$ i. Thus, the degree of cell-size asymmetry resulting from NB divisions may depend on the dosage of the components of one apical pathway when the other is absent or uniformly distributed. In contrast, Miranda localization does not appear to be severely impaired in *G $\gamma$ 1<sup>N159</sup>* and *G $\beta$ 13F* mutants until late embryonic stages, indicating that the polarized Baz–DaPKC activity in these mutants is sufficient to localize Miranda. Therefore, full asymmetry in daughter cell size may require relatively higher levels of Baz–DaPKC activity than polarized distribution of cell-fate determinants does.

In *G $\gamma$ 1<sup>N159</sup>* and *G $\beta$ 13F* mutants, Insc has a different distribution than the other components of the Baz–DaPKC pathway. In most of these mutant NBs, Insc distributes broadly to

both the cytoplasm and the cortex in a slightly asymmetric way, but Baz, DaPKC, and DmPar-6 localize asymmetrically in the cortex. The cytoplasmic distribution of Insc is also slightly asymmetric in *pins* mutant NBs (Fig. 5). It is not known whether cytoplasmic Insc is functional. Interestingly, Insc distribution often appears to correlate better with the asymmetry in daughter cell size than do the other components of the Baz–DaPKC pathway in *G $\gamma$ 1<sup>N159</sup>* and *G $\beta$ 13F* mutants: in most telophase NBs that are cleaving into two equal daughters, DaPKC and DmPar-6 are excluded from the daughter GMC, but Insc tends to distribute evenly to both daughter cells (Fig. S2). This occurs also in *pins* mutants, in which  $\sim$ 15% of NBs divide equally but most NBs divide unequally (Cai et al., 2003). In *pins* NBs cleaving equally, Insc is found equally in the cytoplasm of both daughter cells, but DaPKC and DmPar-6 remain in the newly forming NB; in unequally dividing NBs, all three components are found preferably on the NB side (unpublished data). These observations raise the intriguing possibility that Insc has more important roles in the generation of spindle asymmetry than do the other components of the Baz–DaPKC pathway. Because the absence of Baz results in mislocalization of Insc and vice versa, it is technically difficult to discriminate Insc-specific from Baz-specific functions. It may be Insc or some unknown Insc-associating effectors, rather than Baz, that functions in parallel with Pins–G $\alpha$ i in the establishment of cell-size asymmetry.

#### Pins–G $\alpha$ i and Baz–DaPKC pathways have both overlapping and distinct functions

The question of whether the two apical pathways have redundant functions in aspects of NB division other than cell-size asymmetry has been elusive. In this paper, examination of *G $\gamma$ 1<sup>N159</sup>* and *G $\beta$ 13F* mutant NBs, as well as those overexpressing *baz*, suggest that the asymmetric localization of Miranda depends solely on polarized Baz activity and not on Pins–G $\alpha$ i function. Miranda always distributes on the cortical side opposite to Baz in these mutants and in the wild-type. This also occurs for sensory precursor cells in the peripheral nervous system: in sensory precursory cell division Insc is not expressed, and Pins and Baz distribute on cortical sides opposite to each other, unlike in NBs; however, both Miranda and Numb localize to the cortex opposite Baz, as seen in NBs (unpublished data; Bellaiche et al., 2001).

A previous work showed that phosphorylation of the Lethal (2) giant larvae protein by DaPKC directs the localization of cell-fate determinants to the basal cell cortex (Betschinger et al., 2003). When *baz* is overexpressed in NBs, ectopically distributed Baz excludes Miranda from the Baz region and DaPKC colocalizes with the ectopic Baz, as shown in this work (Fig. 5). In contrast, a decrease in Baz activity in the wild-type results in cytoplasmic localization of DaPKC and uniform cortical distribution of Miranda. All these findings suggest that the Baz-directed localization of DaPKC excludes Miranda from the apical cortex via Lethal (2) giant larvae phosphorylation. In the absence of Baz, Miranda is eventually concentrated to the budding GMC during telophase by unknown mechanisms, a phenomenon called “telophase rescue” (Schober et al., 1999). We observed that this phenomenon did not occur by depleting both *baz* activity and G $\beta$  $\gamma$  signaling (Fig. 2 D; Fuse et al.,



2003), suggesting that telophase rescue involves G $\beta\gamma$  signaling or asymmetric Pins–G $\alpha$ i localization (Yu et al., 2003).

The absence of any single component of the apical complex has the same effect on spindle orientation during NB division, which is normally perpendicular to the apical–basal axis (Kraut et al., 1996; Kuchinke et al., 1998; Wodarz et al., 1999, 2000; Schaefer et al., 2000; Yu et al., 2000, 2003; Petronczki and Knoblich, 2001). Thus, proper orientation of the spindle has been thought to require all the apical components. However, our observations on epithelial cells and mitotic domain 9 cells (summarized in Fig. 7 A) indicated that the spindle always points to the location of Pins when Pins is localized in the cell (Fig. 6). This alignment of the spindle toward Pins occurs irrespective of the localization of the Baz–pathway components. For instance, wild-type epithelial cells divide parallel (Pins direction) but not perpendicular to the apical–basal axis (Baz direction); so do most epithelial cells and mitotic domain 9 cells in *G $\beta$ 13F* and *G $\gamma$ 1* mutants. Therefore, the Pins–G $\alpha$ i pathway, rather than the Baz–DaPKC complex, is likely to play a dominant role in controlling spindle orientation.

In most NBs in *pins*, *G $\beta$ 13F*, and *G $\gamma$ 1* mutants, the spindle is oriented in the direction of Baz localization and therefore follows the localization of the cell-fate determinants. This coincidence results in the determinants' virtually normal segregation to one daughter cell despite the random orientation of division. Thus, only when Pins–G $\alpha$ i are absent or uniformly distributed in NBs, polar Baz activity appears to be capable of directing spindle orientation. Alternatively, the mitotic spindle may position the Baz–DaPKC complex over one spindle pole.

In the NB in which the Baz–DaPKC pathway is depleted, Pins–G $\alpha$ i can still localize asymmetrically and orient the spindle (Yu et al., 2000, 2003). Interestingly, the Pins crescent forms in random orientations in this situation, leading to random spindle orientation. This fact suggests that the Baz–DaPKC complex or its combination with Pins–G $\alpha$ i is necessary to orient the Pins–G $\alpha$ i crescent in the apical direction of the NB, raising an intriguing possibility that there are unknown mechanisms by which formation of the apical complex occurs on the apical side. This postulated mechanism may involve interactions with neighboring epithelial cells.

What is the molecular mechanism by which Pins–G $\alpha$ i orient the spindle? It is interesting to assume that Pins has the ability to attract the spindle pole. This idea is consistent with previous evidence (Yu et al., 2000; Schaefer et al., 2001); although epithelial cells do not normally express Insc, its ectopic expression in these cells recruits Pins–G $\alpha$ i to the apical cortex and reorients the mitotic spindle in the apical–basal direction. The *C. elegans* homologues of Pins, GPR-1/GPR-2, interact with G $\alpha$ i/G $\alpha$ o and a coiled-coil protein, LIN-5, which is required for GPR-1/GPR-2 localization (Gotta et al., 2003; Srinivasan et al., 2003). All these molecules are indeed involved in the regulation of forces attracting spindles during early cleavages. Although Lin-5 has no obvious homologue in other species, functional homologues may regulate Pins localization and/or the connection between the spindle pole and Pins in *Drosophila*. Furthermore, the *C. elegans* gene *ric-8*, which interacts genetically with a G $\alpha$ o gene, is also required for embryonic spindle positioning

(Miller and Rand, 2000). Its homologue in mammals acts as a guanine nucleotide exchange factor for G $\alpha$ o, G $\alpha$ q, and G $\alpha$ i (Tall et al., 2003). An analysis of the *Drosophila* RIC-8 homologue may give insight into the mechanisms by which Pins–G $\alpha$ i regulate spindle orientation.

## Materials and methods

### Genetics

The *N159* mutant of *Drosophila* was identified among 4404 ethylmethane sulfonate–induced zygotic-lethal mutants on the second chromosome. The mutant was mapped to the cytological interval 44D–F, based on its lethality over the deficiency, Df(2R)H3E1, which uncovers the *G $\gamma$ 1* gene (Ray and Ganguly, 1992, 1994). Sequencing the *N159* genomic DNA revealed that the *G $\gamma$ 1* gene has a single C to T nucleotide change, which inserts a stop codon into the *G $\gamma$ 1* protein at the position of amino acid 56. Germ-line clones were made by the FLP–DFS technique (Chou and Perrimon, 1992). The following mutants were also used: *G $\beta$ 13F<sup>Δ13</sup>* (Fuse et al., 2003), *Gai<sup>P8</sup>* (Yu et al., 2003), and *pins<sup>P62</sup>* (Yu et al., 2000).

### Transgenic flies and RNA interference

pUAST vectors (Brand and Perrimon, 1993) containing *MFLAG-G $\gamma$ 1*, *MFLAG-G $\gamma$ 1C67S*, and *MFLAG-G $\gamma$ 1<sup>N159</sup>* were constructed, and fly strains carrying these constructs were established. *G $\gamma$ 1C67S*, which encodes a single cysteine to serine change at amino acid 67, was made by PCR-based site-directed mutagenesis. For phenotype-rescue experiments, *UAS-MFLAG-G $\gamma$ 1*, *UAS-MFLAG-G $\gamma$ 1C67S*, and *UAS-MFLAG-G $\gamma$ 1<sup>N159</sup>* were driven by maternal Gal4 V32 (a gift from D. St. Johnston, Wellcome/CRC Institute, Cambridge, UK) in *G $\gamma$ 1<sup>N159</sup>* germline clone embryos. The same driver was used to overexpress *UAS-baz* (a gift from A. Wodarz, Institute for Genetics, Heinrich-Heine University Dusseldorf, Dusseldorf, Germany). For RNA interference experiments (Kennerdell and Carthew, 1998), embryos were injected with *baz* dsRNA and were allowed to develop until the appropriate stages.

### Immunohistochemistry

Embryos were fixed in 4% PFA for 20 min. For  $\alpha$ -tubulin staining, embryos were fixed in 38% formaldehyde for 1 min (Fuse et al., 2003). The following antibodies were used: anti-Miranda (Ikeshima-Kataoka et al., 1997), anti-G $\beta$ 13F (Fuse et al., 2003), anti-Baz (Ohshiro et al., 2000), anti-PKC $\zeta$  C20 (Santa Cruz Biotechnology, Inc.), anti-DmPar-6 (rabbit IgG against COOH-terminal peptide TIMASDVKDGVLHL), anti-Insc (a gift from W. Chia, MRC Center for Developmental Neurobiology, King's College, London, UK), anti-Cen190 BX63 (a gift from D.M. Glover, University of Cambridge, Cambridge, UK), anti-Pins (a gift from W. Chia), anti-G $\alpha$ i (a gift from X. Yang, Institute of Molecular and Cell Biology, Singapore), anti-neurotactin BP106 (Developmental Studies Hybridoma Bank), anti-phosphohistone H3 (Upstate Biotechnology), anti- $\beta$  galactosidase (Cappel and Promega), anti- $\alpha$ -tubulin (DM1A; Sigma-Aldrich), and anti-FLAG (Sigma-Aldrich). Cy3- or Alexa Fluor 488–conjugated secondary antibodies were obtained from Jackson Laboratories or Molecular Probes, respectively. DNA was stained with TOTO-3 (Molecular Probes). A confocal microscope (BioRad Radiance 2000) was used to acquire images which were processed with Adobe PhotoShop.

### In situ hybridization

In situ hybridization was done as described previously (Tautz and Pfeifle, 1989) by using a digoxigenin-labeled DNA probe containing the coding region of the *G $\gamma$ 1* transcript.

### Coimmunoprecipitation and Western blotting

Fly embryos overproducing MFLAG-G $\gamma$ 1 and MFLAG-Miranda (Ikeshima-Kataoka et al., 1997) under control of the maternal GAL4 V32, as well as wild-type embryos, were mixed with a fivefold volume of lysis buffer (50 mM Tris HCl, pH 8.0, 150 mM NaCl, 1 mM EDTA, 1% Triton X-100, and protease inhibitor cocktail), purchased from Sigma-Aldrich, for 30 min at 4°C. The embryo lysates were centrifuged at maximum speed in a microcentrifuge for 30 min. The supernatants were immunoprecipitated with anti-FLAG antibodies and protein G beads (Amersham Biosciences). Beads were washed five times in the lysis buffer. Bound proteins were analyzed by Western blots with anti-G $\beta$ 13F.

To compare the amount of G $\alpha$ i and G $\beta$ 13F protein between wild-type and *G $\gamma$ 1* mutant embryos, the extracts from wild-type and *G $\gamma$ 1<sup>N159</sup>* germline clone embryos (0–16 h after egg laying) were analyzed by Western

blots with anti-G $\alpha$ i and anti-G $\beta$ 13F. Anti- $\alpha$ -tubulin was used as a control to normalize these extracts.

### Online supplemental material

Fig. S1 shows that the expression of the *G $\gamma$ 1* transgene in *G $\gamma$ 1<sup>N159</sup>* mutants restores the asymmetric cell division of NBs and the cortical localization of G $\beta$ 13F. Fig. S2 shows the distribution of DaPKC and Insc in telophase NBs in *G $\gamma$ 1<sup>N159</sup>* and *G $\beta$ 13F* mutants. Online supplemental material is available at <http://www.jcb.org/cgi/content/full/jcb.200309162/DC1>.

We thank W. Chia, A. Wodarz, X. Yang, the Developmental Studies Hybridoma Bank, and the Bloomington Stock Center for providing flies and antibodies. We also thank M. Saito for technical assistance, and W. Chia, T. Ohshiro, and T. Ishiki for discussions and comments on the manuscript.

This work was supported by grants-in-aid for Science Research from the Ministry of Education, Science, Sports, and Culture of Japan and by Core Research for Evolution Science and Technology for the Japan Science and Technology Corporation.

Submitted: 26 September 2003

Accepted: 20 January 2004

## References

- Bellaiche, Y., A. Radovic, D.F. Woods, C.D. Hough, M.L. Parmentier, C.J. O'Kane, P.J. Bryant, and F. Schweisguth. 2001. The partner of *inscuteable*/discs-large complex is required to establish planar polarity during asymmetric cell division in *Drosophila*. *Cell* 106:355–366.
- Betschinger, J., K. Mechtler, and J.A. Knoblich. 2003. The Par complex directs asymmetric cell division by phosphorylating the cytoskeletal protein Lgl. *Nature* 422:326–330.
- Brand, A.H., and N. Perrimon. 1993. Targeted gene expression as a means of altering cell fates and generating dominant phenotypes. *Development* 118:401–415.
- Cai, Y., F. Yu, S. Lin, W. Chia, and X. Yang. 2003. Apical complex genes control mitotic spindle geometry and relative size of daughter cells in *Drosophila* neuroblast and pI asymmetric divisions. *Cell* 112:51–62.
- Campos-Ortega, J.A. 1995. Genetic mechanisms of early neurogenesis in *Drosophila melanogaster*. *Mol. Neurobiol.* 10:75–89.
- Chia, W., and X. Yang. 2002. Asymmetric division of *Drosophila* neural progenitors. *Curr. Opin. Genet. Dev.* 12:459–464.
- Chou, T.B., and N. Perrimon. 1992. Use of a yeast site-specific recombinase to produce female germline chimeras in *Drosophila*. *Genetics* 131:643–653.
- Doe, C.Q., and B. Bowerman. 2001. Asymmetric cell division: fly neuroblast meets worm zygote. *Curr. Opin. Cell Biol.* 13:68–75.
- Fuse, N., K. Hisata, A.L. Katzen, and F. Matsuzaki. 2003. Heterotrimeric G proteins regulate daughter cell size asymmetry in *Drosophila* neuroblast divisions. *Curr. Biol.* 13:947–954.
- Gotta, M., Y. Dong, Y.K. Peterson, S.M. Lanier, and J. Ahringer. 2003. Asymmetrically distributed *C. elegans* homologs of AGS3/PINS control spindle position in the early embryo. *Curr. Biol.* 13:1029–1037.
- Hirata, J., H. Nakagoshi, Y. Nabeshima, and F. Matsuzaki. 1995. Asymmetric segregation of the homeodomain protein Prospero during *Drosophila* development. *Nature* 377:627–630.
- Horvitz, H.R., and I. Herskowitz. 1992. Mechanisms of asymmetric cell division: two Bs or not two Bs, that is the question. *Cell* 68:237–255.
- Ikeshima-Kataoka, H., J.B. Skeath, Y. Nabeshima, C.Q. Doe, and F. Matsuzaki. 1997. Miranda directs Prospero to a daughter cell during *Drosophila* asymmetric divisions. *Nature* 390:625–629.
- Jan, Y.N., and L.Y. Jan. 2001. Asymmetric cell division in the *Drosophila* nervous system. *Nat. Rev. Neurosci.* 2:772–779.
- Kaltschmidt, J.A., and A.H. Brand. 2002. Asymmetric cell division: microtubule dynamics and spindle asymmetry. *J. Cell Sci.* 115:2257–2264.
- Kaltschmidt, J.A., C.M. Davidson, N.H. Brown, and A.H. Brand. 2000. Rotation and asymmetry of the mitotic spindle direct asymmetric cell division in the developing central nervous system. *Nat. Cell Biol.* 2:7–12.
- Kennerdell, J.R., and R.W. Carthew. 1998. Use of dsRNA-mediated genetic interference to demonstrate that *frizzled* and *frizzled 2* act in the *wingless* pathway. *Cell* 95:1017–1026.
- Knoblich, J.A. 2001. Asymmetric cell division during animal development. *Nat. Rev. Mol. Cell Biol.* 2:11–20.
- Knoblich, J.A., L.Y. Jan, and Y.N. Jan. 1995. Asymmetric segregation of Numb and Prospero during cell division. *Nature* 377:624–627.
- Knust, E., and O. Bossinger. 2002. Composition and formation of intercellular junctions in epithelial cells. *Science* 298:1955–1959.
- Kraut, R., and J.A. Campos-Ortega. 1996. *inscuteable*, a neural precursor gene of *Drosophila*, encodes a candidate for a cytoskeleton adaptor protein. *Dev. Biol.* 174:65–81.
- Kraut, R., W. Chia, L.Y. Jan, Y.N. Jan, and J.A. Knoblich. 1996. Role of *inscuteable* in orienting asymmetric cell divisions in *Drosophila*. *Nature* 383:50–55.
- Kuchinke, U., F. Grawe, and E. Knust. 1998. Control of spindle orientation in *Drosophila* by the Par-3-related PDZ-domain protein Bazooka. *Curr. Biol.* 8:1357–1365.
- Lu, B., M. Rothenberg, L.Y. Jan, and Y.N. Jan. 1998. Partner of Numb colocalizes with Numb during mitosis and directs Numb asymmetric localization in *Drosophila* neural and muscle progenitors. *Cell* 95:225–235.
- Matsuzaki, F. 2000. Asymmetric division of *Drosophila* neural stem cells: a basis for neural diversity. *Curr. Opin. Neurobiol.* 10:38–44.
- Miller, K.G., and J.B. Rand. 2000. A role for RIC-8 (Synembryn) and GOA-1 (G(o) $\alpha$ ) in regulating a subset of centrosome movements during early embryogenesis in *Caenorhabditis elegans*. *Genetics* 156:1649–1660.
- Ohshiro, T., T. Yagami, C. Zhang, and F. Matsuzaki. 2000. Role of cortical tumour-suppressor proteins in asymmetric division of *Drosophila* neuroblast. *Nature* 408:593–596.
- Parmentier, M.L., D. Woods, S. Greig, P.G. Phan, A. Radovic, P. Bryant, and C.J. O'Kane. 2000. Rapsynoid/partner of *inscuteable* controls asymmetric division of larval neuroblasts in *Drosophila*. *J. Neurosci.* 20:RC84.
- Petronczki, M., and J.A. Knoblich. 2001. DmPAR-6 directs epithelial polarity and asymmetric cell division of neuroblasts in *Drosophila*. *Nat. Cell Biol.* 3:43–49.
- Ray, K., and R. Ganguly. 1992. The *Drosophila* G protein  $\gamma$  subunit gene (*D-G $\gamma$ 1*) produces three developmentally regulated transcripts and is predominantly expressed in the central nervous system. *J. Biol. Chem.* 267:6086–6092.
- Ray, K., and R. Ganguly. 1994. Organization and expression of the *Drosophila melanogaster D-G $\gamma$ 1* gene encoding the G-protein  $\gamma$  subunit. *Gene* 148:315–319.
- Rhyu, M.S., L.Y. Jan, and Y.N. Jan. 1994. Asymmetric distribution of numb protein during division of the sensory organ precursor cell confers distinct fates to daughter cells. *Cell* 76:477–491.
- Schaefer, M., A. Shevchenko, and J.A. Knoblich. 2000. A protein complex containing *inscuteable* and the G $\alpha$ -binding protein Pins orients asymmetric cell divisions in *Drosophila*. *Curr. Biol.* 10:353–362.
- Schaefer, M., M. Petronczki, D. Dorner, M. Forte, and J.A. Knoblich. 2001. Heterotrimeric G proteins direct two modes of asymmetric cell division in the *Drosophila* nervous system. *Cell* 107:183–194.
- Schober, M., M. Schaefer, and J.A. Knoblich. 1999. Bazooka recruits *inscuteable* to orient asymmetric cell divisions in *Drosophila* neuroblasts. *Nature* 402:548–551.
- Schulz, S., A. Huber, K. Schwab, and R. Paulsen. 1999. A novel G $\gamma$  isolated from *Drosophila* constitutes a visual G protein  $\gamma$  subunit of the fly compound eye. *J. Biol. Chem.* 274:37605–37610.
- Shen, C.P., L.Y. Jan, and Y.N. Jan. 1997. Miranda is required for the asymmetric localization of Prospero during mitosis in *Drosophila*. *Cell* 90:449–458.
- Spana, E.P., and C.Q. Doe. 1995. The prospero transcription factor is asymmetrically localized to the cell cortex during neuroblast mitosis in *Drosophila*. *Development* 121:3187–3195.
- Srinivasan, D.G., R.M. Fisk, H. Xu, and S. van den Heuvel. 2003. A complex of LIN-5 and GPR proteins regulates G protein signaling and spindle function in *C. elegans*. *Genes Dev.* 17:1225–1239.
- Tall, G.G., A.M. Krumin, and A.G. Gilman. 2003. Mammalian Ric-8A (synembryn) is a heterotrimeric G $\alpha$  protein guanine nucleotide exchange factor. *J. Biol. Chem.* 278:8356–8362.
- Tautz, D., and C. Pfeifle. 1989. A non-radioactive in situ hybridization method for the localization of specific RNAs in *Drosophila* embryos reveals translational control of the segmentation gene hunchback. *Chromosoma* 98:81–85.
- Wodarz, A., A. Ramrath, U. Kuchinke, and E. Knust. 1999. Bazooka provides an apical cue for *inscuteable* localization in *Drosophila* neuroblasts. *Nature* 402:544–547.
- Wodarz, A., A. Ramrath, A. Grimm, and E. Knust. 2000. *Drosophila* atypical protein kinase C associates with Bazooka and controls polarity of epithelia and neuroblasts. *J. Cell Biol.* 150:1361–1374.
- Yu, F., X. Morin, Y. Cai, X. Yang, and W. Chia. 2000. Analysis of partner of *inscuteable*, a novel player of *Drosophila* asymmetric divisions, reveals two distinct steps in *inscuteable* apical localization. *Cell* 100:399–409.
- Yu, F., Y. Cai, R. Kaushik, X. Yang, and W. Chia. 2003. Distinct roles of G $\alpha$ i and G $\beta$ 13F subunits of the heterotrimeric G protein complex in the mediation of *Drosophila* neuroblast asymmetric divisions. *J. Cell Biol.* 162:623–633.